Published in final edited form as:

Gene Ther. 2010 January ; 17(1): 95–104. doi:10.1038/gt.2009.117.

PDGF-B Gene Therapy Accelerates Bone Engineering and Oral Implant Osseointegration

Po-Chun Chang[1,2,*], **Yang-Jo Seol**[1,3,*], **Joni A Cirelli**[1,4], **Gaia R. Pellegrini**[1,5], **Qiming Jin**[1], **Lea M. Franco**[1], **Steven A. Goldstein**[2,4], **Lois A. Chandler**[7], **Barbara Sosnowski**[7], and **William V. Giannobile**[1,2]

[1]Department of Periodontics and Oral Medicine, School of Dentistry, University of Michigan, Ann Arbor, MI, USA 48109

[2]Department of Biomedical Engineering, College of Engineering, University of Michigan, Ann Arbor, MI, USA 48109

[3]Department of Periodontology, School of Dentistry, Seoul National University, Seoul, Korea

[4]Department of Periodontology, School of Dentistry at Araraquara, State University of São Paulo, Araraquara, SP, Brazil

[5]Department of Periodontology, University of Milan, Milan, Italy

[6]Department of Orthopaedic Surgery, School of Medicine, University of Michigan, Ann Arbor, MI, USA 48109

[7]Tissue Repair Company, San Diego, CA USA

Abstract

Platelet-derived growth factor-BB (PDGF-BB) stimulates repair of healing-impaired chronic wounds such as diabetic ulcers and periodontal lesions. However, limitations in predictability of tissue regeneration occur due in part to transient growth factor bioavailability *in vivo*. Here, we report that gene delivery of PDGF-B stimulates repair of oral implant extraction socket defects. Alveolar ridge defects were created in rats and were treated at the time of titanium implant installation with a collagen matrix containing an adenoviral (Ad) vector encoding PDGF-B (5.5×10^8 or 5.5×10^9 pfu/ml), Ad encoding luciferase (Ad-Luc; 5.5×10^9 pfu/ml; control) or recombinant human PDGF-BB protein (rhPDGF-BB, 0.3 mg/ml). Bone repair and osseointegration were measured via backscattered SEM, histomorphometry, microcomputed tomography, and biomechanical assessments. Further, a panel of local and systemic safety assessments was performed. Results demonstrated bone repair was accelerated by Ad-PDGF-B

Correspondence should be addressed to W.V.G. (william.giannobile@umich.edu): William V. Giannobile, University of Michigan, 1011 N. University Ave., Ann Arbor, MI 48109, Tel: (734) 764-1562, Fax: (734) 763-5503.

*These authors contributed equally to this work.

Conflict of interest: Lois A. Chandler and Barbara Sosnowski are employees of Tissue Repair Company. Steven A. Goldstein may receive royalties if as distributed by the University of Michigan, and the University of Michigan may benefit from the subject of this paper, as a result of the technology that was licensed to Tissue Repair Company. William Giannobile has financial interest in BioMimetic Therapeutics, Inc.

and rhPDGF-BB delivery compared to Ad-Luc, with the high dose of Ad-PDGF-B more effective than the low dose. No significant dissemination of the vector construct or alteration of systemic parameters was noted. In summary, gene delivery of Ad-PDGF-B demonstrates regenerative and safety capabilities for bone tissue engineering and osseointegration in alveolar bone defects comparable to rhPDGF-BB protein delivery *in vivo*.

Keywords

dental implant; platelet-derived growth factor; gene therapy; regenerative medicine; virus delivery

Introduction

Oral implants are widely accepted in dental medicine as a reconstructive treatment modality for tooth replacement due to disease, injury, or congenital defects. In clinical situations exhibiting limited alveolar bone availability, growth factor application has been advocated to improve osteogenesis and osseointegration 1. However, as a result of the transient action and the high degradation rate of recombinant proteins *in vivo* 2, the sustained bioactivity of gene therapy vectors has been purported to be an effective alternative for the delivery of growth factor proteins 3,4. Adenoviral vectors (Ad) have been shown to exhibit a high *in vivo* transduction efficiency 5 with a relatively short expression period compared with other viral-based gene delivery methods, and their effectiveness for promoting initial wound healing without eliciting long-term health concerns in wound healing models 6,7.

Platelet-derived growth factor (PDGF) is a potent mitogen that facilitates wound healing 8 and stimulates bone repair by expanding osteoblastic precursor cells 9,10. PDGF-BB is FDA-approved for use in the treatment of localized periodontal defects and diabetic ulcers 11-13. Ad-mediated PDGF-B (Ad-PDGF-B) gene delivery has been shown to enhance periodontal tissue regeneration of tooth-supporting wounds 6,14.

Limited information is available regarding the potential of PDGF-BB on promoting osseointegration of oral implants. In addition, the influence of PDGF-B on the mechanical integrity of an implant interface is unknown. The purpose of this study was to investigate the effects of rhPDGF-BB and Ad-PDGF-B delivered in a collagen matrix on the osteogenesis and osseointegration of dental implants in an *in vivo* osseointegration model in the rat. This approach demonstrates the ability of Ad-PDGF-B to accelerate oral implant osseointegration. The data support the concept that Ad-PDGF-B gene delivery may be an effective and safe mode of therapy comparable to PDGF-BB application to promote dental implant osseointegration and oral bone repair.

Materials and Methods

Experimental Design

A total of 100 male Sprague-Dawley rats were used in this study and the general timeline is shown in Fig 1a. Based on the power analysis calculations from a similar study, 6∼8 animals were analyzed per treatment per time point14. A rat dental implant osseointegration wound model was modified for the *in vivo* experiments. Eighty-two animals were utilized

for evaluating the effects of osseointegration, with 3 timepoints (day 10, 14, and 21) and 4 treatment groups (5.5×10^9 pfu/ml Ad-Luc as the control group, 5.5×10^8 pfu/ml Ad-PDGF-BB, 5.5×10^9 pfu/ml Ad-PDGF-BB, and 0.3 mg/ml rhPDGF-BB) evaluated. Additionally, 18 animals were equally divided into 3 treatment groups (collagen matrix alone as the control group, 5.5×10^8 pfu/ml Ad-PDGF-BB, 5.5×10^9 pfu/ml Ad-PDGF-BB) and used for determining the preclinical safety profile, with assessments performed on these same animals over an observation period of 35 days.

Adenoviral Vectors and Recombinant Protein

Ad-PDGF-B (E1-, E3-deleted adenovirus serotype 5 encoding human platelet-derived growth factor-B) and Ad-Luc (E1-, E3-deleted adenovirus serotype 5 encoding firefly luciferase) have been previously described 6. In both vectors, transgene expression is under control of the CMV promoter. Titers of virus stocks were determined on embryonic kidney 293 cells by plaque assay and expressed as the particle number per milliliter 7. The rhPDGF-BB was purchased from Biomimetic Therapeutics, Inc. (Franklin, TN, USA) at a working concentration of 0.5 mg/ml.

Preparation of Vector/Protein-Gene Activated Matrix

Ad-PDGF-B, A d-Luc, and rhPDGF-BB were dialyzed into GTS buffer (2.5% glycerol, 25 mM NaCl, 20 mM Tris, pH 8.0) and formulated in bovine fibrillar type I collagen matrix (Matrix Pharmaceutical Inc., Fremont, CA, USA) at a final concentration of 2.6%.

Animal model for evaluating therapeutic effects

All animal procedures followed the guidelines from the Committee on Use and Care of Animals of the University of Michigan. The maxillary first molars were extracted bilaterally 4 weeks prior to dental implant installation. After healing, an osteotomy was created using a custom drill-bit by a single surgeon (YJS). The drill-bit was designed with a 0.95 mm diameter, 1 mm long-apical portion and a 2.2 mm diameter, 1 mm long at the coronal aspect (Fig. 1b). The apical part of the drill created an osteotomy for initial fixation and the coronal part of the drill created a circumferential osseous defect prior to dental implant installation. A custom cylinder-type titanium mini-implant (kind gift of Institut Straumann AG, Basel, Switzerland), 1 mm-in-diameter and 2 mm-in-depth, was press-fit into the surgically-created socket (Fig 1b). The remaining defect was then filled with the type I collagen matrix containing 5.5×10^9 pfu/ml Ad-Luc, 5.5×10^8 pfu/ml Ad-PDGF-B, 5.5×10^9 pfu/ml Ad-PDGF-B, or 0.3 mg/ml rhPDGF-BB (Fig 1b). Ad-Luc has not previously exhibited biological activities in dentoalveolar defects 14 and served as control group in this study. The surgical area was covered by gingival tissue and reapproximated using butyl cyanoacrylate (Periacryl®, Glustitch Inc., Point Roberts, WA, USA). The vital fluorochrome dye, calcein (10 mg/kg), was injected intra-muscularly after 3 days, and antibiotics (268 mg/L ampicillin in 5% dextrose water) were provided during the first 7 days post-operation.

Backscattered SEM and histology

Coded maxillae containing the implants were harvested upon sacrifice, with one side of maxillae taken for backscattered SEM and histology while the contralateral maxillae were

used for biomechanical assessments (*see following section*). The specimens were fixed in 50% ethanol for at least 72 hours and subsequently embedded in epoxy resin. The specimens were then sectioned in the longitudinal direction relative to the implants using a diamond saw blade (Crystalite Co., Westerville OH, USA), then polished to achieve a 50-100 μm final thickness. The tissue mineralization was evaluated under the backscattered mode on Qanta F1B SEM with 45× magnification, calibrated with aluminum and carbon discs 15, and transferred to physical density using bone substitute radiographic phantoms (Gammex Inc., Middleton WI, USA). The photographs were then segmented and threshholded by Otsu's adaptive technique16. To eliminate any metal scattering effect, the measured bone-implant interface was defined as the horizontal distance 5 μm from the outermost homogenous high-intensity area. The defect borders were projected using the calcein fluorescent images. Bone-area fractions (BAF, the ratio of newly-formed bone in the defect to the entire defect area) and Tissue mineral density within the defect (TMD, the average grayscale level of mineralized tissue within the defect area) were measured from backscattered SEM images. Next, histologic staining by methylene blue was performed, with the acid fuschin utilized as the counterstain 17. Bone-implant contact (BIC, the ratio of the length of bone contacting the titanium to the entire length of titanium interface with the defect area) and defect fill (DF, the ratio of bone-occupied area to the entire defect area) were measured by calibrated examiners PCC and YJS).

Biomechanical, three-dimensional radiographic, and functional evaluations

The remaining maxillae were used for biomechanical and micro-CT evaluation and stored in normal saline at -20°C to preserve the mechanical integrity. After thawing at room temperature, the specimens were rapidly secured in acrylic resin. The mini-implants were meticulously pushed out of each maxilla using an MTS machine (Model 858, Mini-Bionix II, MTS Systems Corp., Eden Prairie, MN, USA) at a constant displacement rate of 0.1 mm/s, while recording the load-displacement relationship of the top of implant was recorded during the push-out procedures. The region from 20% to 80% of the maximum removal load (MRL) was chosen and a linear regression was performed to calculate the interfacial stiffness (IS). A previously described osseointegration index (OI) based on the nature of the bone fail during implant push-out tests was also utilized to further document the interfacial biomechanical behavior (Table S1) 18.

After implant push-out, micro-CT scans were performed using an eXplore Locus SP Micro-CT system (GE HealthCare, London, ON, Canada) and reconstructed to voxel size of $18\times18\times18\ \mu m^3$. The spatial relationship of the mini-implant and surrounding tissues was then analyzed using a customized MATLAB® (Mathworks Inc., Natick, MA, USA) algorithm. The images were segmented with a threshold determined by Otsu's adaptive technique16, and several parameters were quantitatively evaluated within the osseous defect areas: (1) Bone volume fraction (BVF): the volume of mineralized tissue within the osseous wound divided by the volume of osseous wound; (2) Tissue mineral density (TMD): the mineral content of the radiographic-defined mineralized tissue within the osseous wound divided by the volume of osseous wound; (3) Bone mineral density (BMD): the mineral density within the radiographic-defined mineralized tissue in the osseous wound. After micro-CT evaluations, the images were transferred to create a finite element (FE) mesh, and

the functional bone modulus (FBM, referring to the rigidity of bone within the area of interest toward dental implant) and functional composite tissue apparent modulus (FCAM, rigidity of the whole tissue within the area of interest toward dental implant) were generated from previously described simulation procedures 18.

Animal model for safety profile

18 male Sprague-Dawley rats had their first maxillary molars extracted, osseous defect created, and implant placement as previously described.17 The osseous defects were filled with the type I collagen vehicle alone, or containing Ad-PDGF-B (5.5×10^8 or 5.5×10^9 pfu/ml). Another six animals without any surgical treatments were also included to provide baseline parameters. Blood was drawn from rat tail veins at baseline and at 1, 2, 3, 4, 5, 6, 7, 14, 21, 28, and 35 days. Hematological and clinical chemistry parameters (listed in Table 1) were examined at baseline and at 3, 7, 14, 21, 28, and 35 days. Vector dissemination was evaluated for all blood draw time points. Genomic DNA was isolated from 50μl whole blood using QIAamp DNA Blood Mini kit (QIAGEN Inc., Valencia, CA, USA), and quantitative TaqMan PCR was used to determine the copies of Ad-PDGF-B in the bloodstream. The primers used for qPCR bridging the vector backbone and PDGF-B prepro region were: sense -- 5′-GGATCTTCGAGTCGACAAGCTT-3′; anti-sense -- 5′-ATCTCATAAAGCTCCTCGGGAAT-3′; internal fluorogenic probe -- 5′-CGCCCAGCAGCGATTCATGGTGAT-3′. The resulting amplicon was detected by ABI Prism 7700 sequence detection instrument (Applied Biosystems, Foster City, CA, USA), and the thermal condition was: 50°C 2 minutes, 95°C 10 minutes followed by 45 cycles of 95°C 15 seconds and 60°C 1 minute. The assay sensitivity was 30 copies/500ng DNA. There was no cross-reaction with adenoviral vector encoding PDGF-A, PDGF-1308 (dominant-negative, PDGF mutant), bone morphogenetic protein-7, noggin, bone sialoprotein, Ad-Luc, or green fluorescent protein.

Statistical Analysis

One-way ANOVA with Tukey test was utilized to analyze the difference of coded specimens for histomorphometric, backscattered SEM, micro-CT, biomechanical, and functional parameters between PDGF-treated (collagen containing 0.3 mg/ml rhPDGF-BB, 5.5×10^8 or 5.5×10^9 pfu/ml Ad-PDGF-B) and non-PDGF-treated (collagen alone) groups at each time point. For evaluating the safety profile, the difference of vector replicates, hematological and chemical parameters between experimental (collagen containing 5.5×10^8 or 5.5×10^9 pfu/ml Ad-PDGF-B) was evaluated for time-dependent dynamics with control (collagen alone) group using Bonferroni post-tests, and the significance was assessed by repeated-measures ANOVA. The statistical difference was considered with a p value of less than 0.05.

Results

Ad-PDGF-B and rhPDGF-BB enhance osteogenesis *in vivo*

Based on the descriptive histology (Fig 2a), by day 10 a gradual defect resolution was observed over time in all groups. At days 10 and 14, woven bone and primary trabecular

bone were noted at the coronal margin (red asterisks) in Ad-Luc-treated specimens, and thicker bone trabeculae and defect fill were evident in all PDGF-treated specimens (black asterisks in 5.5×10^8 and 5.5×10^9 pfu/ml Ad-PDGF-B, and rhPDGF-BB). Also at day 14, more mature bone apposition and near-complete defect fill was noted for all PDGF-treated specimens (Fig 2a, lower panel). The histomorphometric measurements of the 5.5×10^9 pfu/ml Ad-PDGF-B and rhPDGF-BB groups showed significantly higher bone-implant contact (BIC) than the Ad-Luc group at day 10 ($p<0.05$, Fig. 2b). Further, all PDGF groups revealed higher defect fill (DF) than Ad-Luc at days 10 ($p<0.01$, Fig. 2c) and 14 ($p<0.05$, Fig. 2c). An equivalent defect repair pattern was noted from the backscattered SEM (BS-SEM) images (Fig. 3a). At day 10, BS-SEM measurements also demonstrated a significant difference among all PDGF-treated groups compared with the Ad-Luc-treated group in both bone-area fraction (BAF, $p<0.05$, Fig 3b) and tissue mineral density (TMD, $p<0.05$, Fig 3c). A significant difference between rhPDGF-BB and Ad-Luc in TMD was also noted at day 14 ($p<0.05$, Fig. 3c). Completion of the defect fill was noted in all the animals by day 21, and no significant differences for any BS-SEM or histomorphometric parameters could be found among all the groups (data not shown).

Both Ad-PDGF-B and rhPDGF-BB promote osseointegration

The consequence of push-out testing was reflected from the osseointegration index (OI), with all PDGF-treated specimens showing higher scores than Ad-Luc, with significant differences noted between rhPDGF-BB and Ad-Luc at both days 10 and 14 ($p<0.05$, Fig 4a). PDGF application tended to improve the interfacial stiffness (IS) and maximum removal loading (MRL) compared to the Ad-Luc group. The rhPDGF-BB treatment demonstrated significantly higher interfacial stiffness (IS) than all other groups at days 10 and 14 ($p<0.05$, Figure 4b), and higher maximum removal loading (MRL) than all other groups at day 10 ($p<0.05$, Fig 4c). At day 14, the MRL of rhPDGF-BB was significantly higher compared to both the Ad-Luc and the 5.5×10^9 pfu/ml Ad-PDGF-B groups ($p<0.05$, Fig 4c). Significant improvement of IS using 5.5×10^8 pfu/ml Ad-PDGF-B treatment versus Ad-Luc ($p<0.05$, Fig. 4b) was also seen at day 10. Most day 21 specimens experienced cortical bone fractures during the push-out testing (suggestive of strong osseointegration), and no significant differences among all the groups in IS and OI scores were noted (data not shown).

Micro-CT images were analyzed after implant removal, and both the 5.5×10^9 pfu/ml Ad-PDGF-B and rhPDGF-BB groups displayed significantly higher bone volume fraction (BVF) and tissue mineral density (TMD) than the 5.5×10^8 pfu/ml Ad-PDGF-B and Ad-Luc groups at day 10 ($p<0.05$, Fig. 4d, e). A significant difference in BVF was found between 5.5×10^9 pfu/ml Ad-PDGF-B and Ad-Luc at day 14 ($p<0.05$, Fig 4d). Both the 5.5×10^9 pfu/ml Ad-PDGF-B and rhPDGF-BB groups displayed equivalent extents of functional composite tissue apparent modulus (FCAM), which was significantly stiffer than the 5.5×10^8 pfu/ml Ad-PDGF-B or Ad-Luc groups at day 10 ($p<0.05$, Fig. 4f). At day 14, there were no FCAM differences between any of the treatment groups.

Local delivery of Ad-PDGF-B exhibits acceptable safety profiles *in vivo*

In a separate study of systemic safety, animals were treated with collagen alone (control) or collagen containing Ad-PDGF-B (5.5×10^8 or 5.5×10^9 pfu/ml). Blood samples were taken at

various time points for hematological and clinical chemistry analyses and PCR analyses for vector sequence. All animals survived until the day of sacrifice, with no progressive swelling or symptoms noted. The majority of hematological and clinical chemistry parameters were within their normal ranges with no significant differences between Ad-PDGF-B and collagen only treatments (Tables 1 and 2).

Vector-specific quantitative PCR 6 was performed on blood samples taken (name time points) after treatment. Ad-PDGF-B was not detected in the bloodstream over the 35 day observation period (data not shown).

Discussion

This study demonstrates that both Ad-PDGF-B gene and rhPDGF-BB protein delivery promotes the acceleration of neo-osteogenesis of peri-implant bony defects *in vivo*. The affect on bone apposition was examined through DF from histomorphometry (Fig 2c), BAF from BS-SEM (Fig 3b), and BVF from micro-CT (Fig 4d). From these results, all treatment groups, especially the 5.5×10^9 pfu/ml Ad-PDGF-B and rhPDGF-BB groups showed significantly greater bone formation compared to the Ad-Luc vector control group at 10 days. Regarding bone maturation, the Ad-Luc-treated defects showed sparse and limited new bone formation and slower bone formation within the defect area compared to the other three groups. By day 14, in the Ad-Luc group, new bone near the base of the defect (Fig. 2a) showed thick trabeculae and bone marrow formation suggesting greater maturation, whereas the thin trabeculae and primary woven bone-like structures at the coronal portion of the defects suggests early-stage osteogenesis. However, in all PDGF-treated groups, advanced bone maturation throughout the defect area, especially in the higher dose Ad-PDGF-B and rhPDGF-BB groups, indicates that new bone formation initiated earlier in those two groups compared to controls. Taken together, these results strongly suggest that PDGF delivery, via both the protein and the gene delivery vector, significantly accelerated and enhanced new bone formation in the peri-implant defects, and the higher dose of Ad-PDGF-B showed more favorable results than lower dosage suggesting a dose-dependent effect on osseointegration.

We also presented FCAM predicting the functional contribution of the newly-formed bone through the FE optimization procedures 18. FCAM is more correlated to the implant interfacial resistance than any single structural parameter. Significantly higher FCAM from the 5.5×10^9 pfu/ml Ad-PDGF-B and rhPDGF-BB treatments at day 10 indicates that both PDGF protein and gene delivery stimulates not only osteogenesis but also favorable initial implant function.

Two-dimensional and three-dimensional quantification results between rhPDGF-BB and higher dose Ad-PDGF-B were also comparable (Fig 2-4). However, the biomechanical analyses did not show equivalent trends, whereas rhPDGF-BB demonstrated significant improvements versus Ad-Luc for most of the parameters (Fig 4a-c). Although the correlation between implant stability and peri-implant structures had been proven in previous research 19,20, this finding may be due to the different delivery profile of PDGF by either Ad or as a protein. While the initial response to a bolus administration of rhPDGF-

BB may be robust, the protein's short half-life results in rapid degradation within a few days 2, and a decrease in the mitogenic response. In contrast, Ad-PDGF-B delivery demonstrates a delayed PDGF-BB expression profile that gradually decreases to ∼20% of the highest level by day 14 *in vivo* 14. This finding is consistent with a previous report whereby Ad-PDGF-B prolongs PDGF signaling leading to a delay with respect to timing of osteogenic differentiation 21.

PDGF's effects on osseous wound healing have been reported mechanistically in previous investigations. It had been shown that PDGF signaling is important for chemotaxis and proliferation of osteoblasts and fibroblasts 22,23. However, PDGF's ability to induce osteogenic lineage differentiation is less clear. Tokudaga et al. 24 reported PDGFRβ signaling strongly inhibited osteogenic differentiation of mesenchymal stem cells, and Kono et al. 25 further validated that the Erk signaling, which is the subsequent PDGFR pathway, negatively regulated osteogenesis. On the other hand, other evidence implies that PDGF contributes to osteogenic differentiation via a more downstream mechanism. Huang et al. 26 detected PDGF mRNA expression at both the early proliferation stage and a late differentiation stage of osteoprogenitor cells. Furthermore, Ng et al. 27 showed that PDGFR activation was a key step for the osteogenic lineage differentiation of mesenchymal stem cells, while inhibition of PDGFβR resulted in decreased mineralized nodule formation. Kratchmarova et al. 28 reported that PDGF increased new bone formation *in vivo* despite limited influences in osteogenic differentiation *in vitro*. These results imply that the differentiation is promoted at a certain level of expression, such as dose- or time-dependent reactions 22,23. Donatis et al. 22 reported that a higher concentration of PDGF is favorable for mitogenesis and lower doses for cell motility. Hsieh et al. 23 found that pulse application of PDGF enhances bone formation, but prolonged exposure to PDGF limited *in vitro* bone regeneration. Since osteogenesis involves a cascade of events *in vivo*, varying strategies of PDGF delivery must be considered for different indications. Thus, the rhPDGF-BB treatment may be suitable for the needs of rapid bone fill, where it would quickly recruit cells without significantly affecting the time frame of subsequent differentiation (Supplementary Fig. 1a). The higher dose of Ad-PDGF-B may be a better choice for a large wound site (that remains to be tested), in which the sustained PDGF signal would attract cell progenitors for a more extended, but still limited period of time so that the differentiation and maturation would initiate after PDGF signaling subsided (supplementary figure 1b). Given the limited size of the rat maxilla and the high cell proliferative activity, it is necessary to further validate this assumption in a large animal model with more challenging, critical-size defects.

This use of gene therapy introduced a different strategy when compared to traditional scaffold-growth factor delivery. In our approach, the main function of the gene-activated matrix (i.e., collagen matrix) was to mobilize the vector and allow for cell invasion 29. The vector is then actively transfected into the cells, followed by disintegration of capsid, condensed by the adenovirus core proteins to enter the nucleus (<40 nm diameter) for the subsequent expression of the carrier gene 30. Thus, the rate-limiting step of gene delivery was the vector transduction. High levels of adenovirus transduction within the first two weeks of delivery, and favorable regenerative effects have been documented in several

studies 6,14,17. Further efforts on the condensation of adenovirus vector may be beneficial for amplifying the efficiency of the gene therapy 30.

The angiogenic effect of PDGF, which are similar to the effect of vascular endothelial growth factor (VEGF), may also be favorable for osseous wound repair. During wound healing, angiogenesis is an important event for new tissue regeneration (i.e., providing nutrients and essential signals). The PDGFs have a similar structure to VEGF 31, and PDGF-BB enhances fibroblast growth factor-2 (FGF-2) stimulated VEGF release 32. PDGFRβ also has an important role in angiogenesis 33. Therefore, it is reasonable to conclude that PDGF-BB also positively affects angiogenesis and ultimately contributes to bone formation. Considering that dental implant function (with a metallic non-vascularized interface) is largely dependent on the surrounding bone quantity, quality and wound healing microenvironment, these accelerating and enhancing bone formation effects of PDGF may promote greater bone volume for earlier implant placement and loading.

One important consideration with the use of gene therapy vectors is the potential immune response and related sequelae 34,35. In our study, Ad-PDGF-B was delivered in a collagen matrix which potentially masks the host immune function against adenoviral vectors *in vivo* 17,21,29,36. Typically, transformation and self-replication is eliminated by removing the E1- and E3-gene regions of the adenovirus genome 37. We discovered no significant vector dissemination or alteration of hematological and clinical chemistry parameters. Our results demonstrated a favorable preclinical safety profile and was comparable to our previous investigation examining Ad-PDGF-B in periodontal defects6. Furthermore, a non-viral based vector might be an alternative for delivering the PDGF-B gene with minimal safety concerns. However, further efforts on the improvement of efficient delivery and expression of the non-viral vectors is still necessary 38,39.

In summary, this investigation demonstrates the first reported use of Ad-PDGF-B administration to promote alveolar bone repair and osseointegration in alveolar ridge defects. These findings suggest that Ad-PDGF_B stimulates osseointegration that is comparable with delivery of PDGF-BB protein. A good safety profile was demonstrated supportive for extending this approach to large animal model studies examining large critical-size bony defects in the craniofacial complex.

Supplementary Material

Refer to Web version on PubMed Central for supplementary material.

Acknowledgments

The authors thank Valeria Pontelli Navarro Tedeschi for assistance with animal surgeries, Dennis Kayner for assisting removal of the implants, Dr. Noboru Kikuchi for establishing finite element models, and Anna Colvig for performing hematological and clinical chemical examinations. This study was supported in part by the grants from National Institutes of Health (NIH)/National Institute of Dental and Craniofacial Research (NIDCR) (R01-DE13397) and AO Foundation Research Advisory Council (Davos, Switzerland) to WVG.

This study was supported by the grants from NIH/NIDCR (R01-DE13397) and AO Foundation Research Advisory Council (Davos, Switzerland).

References

1. Wikesjo UM, Sorensen RG, Wozney JM. Augmentation of alveolar bone and dental implant osseointegration: clinical implications of studies with rhBMP-2. J Bone Joint Surg Am. 2001; 83-A(1):S136–145. [PubMed: 11314791]
2. Lynch SE, et al. The effects of short-term application of a combination of platelet-derived and insulin-like growth factors on periodontal wound healing. J Periodontol. 1991; 62:458–467. [PubMed: 1920013]
3. Fang J, et al. Stimulation of new bone formation by direct transfer of osteogenic plasmid genes. Proc Natl Acad Sci U S A. 1996; 93:5753–5758. [PubMed: 8650165]
4. Ramseier CA, Abramson ZR, Jin Q, Giannobile WV. Gene therapeutics for periodontal regenerative medicine. Dent Clin North Am. 2006; 50:245–263. ix. [PubMed: 16530061]
5. Ghosh SS, Gopinath P, Ramesh A. Adenoviral vectors: a promising tool for gene therapy. Appl Biochem Biotechnol. 2006; 133:9–29. [PubMed: 16622281]
6. Chang PC, et al. Adenovirus Encoding Human Platelet-Derived Growth Factor-B Delivered to Alveolar Bone Defects Exhibits Safety and Biodistribution Profiles Favorable for Clinical Use. Hum Gene Ther. 2009
7. Gu DL, et al. Adenovirus encoding human platelet-derived growth factor-B delivered in collagen exhibits safety, biodistribution, and immunogenicity profiles favorable for clinical use. Mol Ther. 2004; 9:699–711. [PubMed: 15120331]
8. Barrientos S, et al. Growth factors and cytokines in wound healing. Wound Repair Regen. 2008; 16:585–601. [PubMed: 19128254]
9. Anusaksathien O, et al. Effect of sustained gene delivery of platelet-derived growth factor or its antagonist (PDGF-1308) on tissue-engineered cementum. J Periodontol. 2004; 75:429–440. [PubMed: 15088882]
10. Canalis E, McCarthy TL, Centrella M. Effects of platelet-derived growth factor on bone formation in vitro. J Cell Physiol. 1989; 140:530–537. [PubMed: 2777891]
11. Nevins M, et al. Platelet-derived growth factor stimulates bone fill and rate of attachment level gain: results of a large multicenter randomized controlled trial. J Periodontol. 2005; 76:2205–2215. [PubMed: 16332231]
12. Uhl E, Rosken F, Sirsjo A, Messmer K. Influence of platelet-derived growth factor on microcirculation during normal and impaired wound healing. Wound Repair Regen. 2003; 11:361–367. [PubMed: 12950640]
13. Simion M, Rocchietta I, Monforte M, Maschera E. Three-dimensional alveolar bone reconstruction with a combination of recombinant human platelet-derived growth factor BB and guided bone regeneration: a case report. Int J Periodontics Restorative Dent. 2008; 28:239–243. [PubMed: 18605599]
14. Jin Q, et al. Engineering of tooth-supporting structures by delivery of PDGF gene therapy vectors. Mol Ther. 2004; 9:519–526. [PubMed: 15093182]
15. Traini T, et al. Comparative evaluation of the peri-implant bone tissue mineral density around unloaded titanium dental implants. J Dent. 2007; 35:84–92. [PubMed: 16979279]
16. Otsu N. Threshold Selection Method from Gray-Level Histograms. Ieee Transactions on Systems Man and Cybernetics. 1979; 9:62–66.
17. Dunn CA, et al. BMP gene delivery for alveolar bone engineering at dental implant defects. Mol Ther. 2005; 11:294–299. [PubMed: 15668141]
18. Chang PC, et al. *In vivo* FEA predicts functional oral implant osseointegration. J Dent Res. in press.
19. Gabet Y, et al. Parathyroid hormone 1-34 enhances titanium implant anchorage in low-density trabecular bone: a correlative micro-computed tomographic and biomechanical analysis. Bone. 2006; 39:276–282. [PubMed: 16617039]
20. Ramp LC, Jeffcoat RL. Dynamic behavior of implants as a measure of osseointegration. Int J Oral Maxillofac Implants. 2001; 16:637–645. [PubMed: 11669245]

21. Lin Z, et al. Platelet-derived growth factor-B gene delivery sustains gingival fibroblast signal transduction. J Periodontal Res. 2008; 43:440–449. [PubMed: 18823454]
22. De Donatis A, et al. Proliferation versus migration in platelet-derived growth factor signaling: the key role of endocytosis. J Biol Chem. 2008; 283:19948–19956. [PubMed: 18499659]
23. Hsieh SC, Graves DT. Pulse application of platelet-derived growth factor enhances formation of a mineralizing matrix while continuous application is inhibitory. J Cell Biochem. 1998; 69:169–180. [PubMed: 9548564]
24. Tokunaga A, et al. PDGF receptor beta is a potent regulator of mesenchymal stromal cell function. J Bone Miner Res. 2008; 23:1519–1528. [PubMed: 18410236]
25. Kono SJ, et al. Erk pathways negatively regulate matrix mineralization. Bone. 2007; 40:68–74. [PubMed: 16978937]
26. Huang Z, Nelson ER, Smith RL, Goodman SB. The sequential expression profiles of growth factors from osteoprogenitors [correction of osteroprogenitors] to osteoblasts in vitro. Tissue Eng. 2007; 13:2311–2320. [PubMed: 17523879]
27. Ng F, et al. PDGF, TGF-beta, and FGF signaling is important for differentiation and growth of mesenchymal stem cells (MSCs): transcriptional profiling can identify markers and signaling pathways important in differentiation of MSCs into adipogenic, chondrogenic, and osteogenic lineages. Blood. 2008; 112:295–307. [PubMed: 18332228]
28. Kratchmarova I, et al. Mechanism of divergent growth factor effects in mesenchymal stem cell differentiation. Science. 2005; 308:1472–1477. [PubMed: 15933201]
29. Doukas J, et al. Matrix immobilization enhances the tissue repair activity of growth factor gene therapy vectors. Hum Gene Ther. 2001; 12:783–798. [PubMed: 11339895]
30. Pouton CW, et al. Targeted delivery to the nucleus. Adv Drug Deliv Rev. 2007; 59:698–717. [PubMed: 17681634]
31. Andrae J, Gallini R, Betsholtz C. Role of platelet-derived growth factors in physiology and medicine. Genes Dev. 2008; 22:1276–1312. [PubMed: 18483217]
32. Tokuda H, et al. Potentiation by platelet-derived growth factor-BB of FGF-2-stimulated VEGF release in osteoblasts. J Bone Miner Metab. 2008; 26:335–341. [PubMed: 18600399]
33. Zhang J, et al. Differential roles of PDGFR-{alpha} and PDGFR-{beta} in angiogenesis and vessel stability. Faseb J. 2008 in press.
34. Douglas JT. Adenoviral vectors for gene therapy. Mol Biotechnol. 2007; 36:71–80. [PubMed: 17827541]
35. Hartman ZC, Appledorn DM, Amalfitano A. Adenovirus vector induced innate immune responses: impact upon efficacy and toxicity in gene therapy and vaccine applications. Virus Res. 2008; 132:1–14. [PubMed: 18036698]
36. Sonobe J, et al. Osteoinduction by bone morphogenetic protein 2-expressing adenoviral vector: application of biomaterial to mask the host immune response. Hum Gene Ther. 2004; 15:659–668. [PubMed: 15242526]
37. Wang Y, et al. Characterisation of systemic dissemination of nonreplicating adenoviral vectors from tumours in local gene delivery. Br J Cancer. 2005; 92:1414–1420. [PubMed: 15812558]
38. Paleos CM, Tziveleka LA, Sideratou Z, Tsiourvas D. Gene delivery using functional dendritic polymers. Expert Opin Drug Deliv. 2009; 6:27–38. [PubMed: 19236206]
39. Ditto AJ, Shah PN, Gump LR, Yun YH. Nanospheres Formulated from l-Tyrosine Polyphosphate Exhibiting Sustained Release of Polyplexes and In Vitro Controlled Transfection Properties. Mol Pharm. 2009; 6:986–995. [PubMed: 19341289]

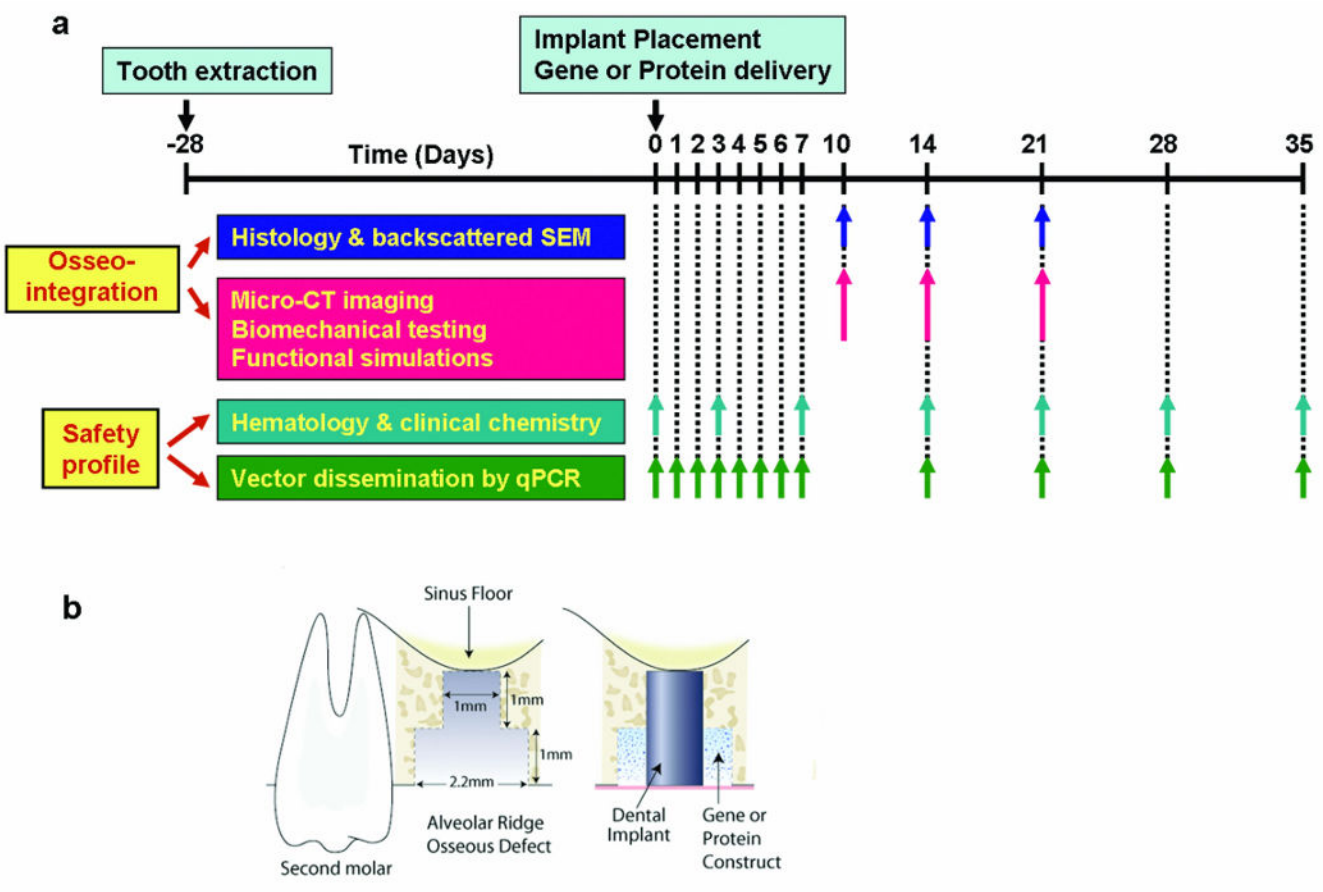

Figure 1. Experimental design (a) and experimental model illustration (b)

Implant surgery was performed four weeks following maxillary first molar extraction. To create a consistent and reproducible defect, custom-made step drills were used. After dental implant placement, the bone defect was filled with 5.5×10^9 pfu/ml Ad-Luc, 5.5×10^8 pfu/ml Ad-PDGF-B, 5.5×10^9 pfu/ml Ad-PDGF-B or 0.3 mg/ml rhPDGF-BB formulated with the collagen matrix for evaluating osseointegration (n=6-8/group/time point). Histomorphometric and backscattered SEM measurements were done at days 10, 14 and 21 after implant installation, and three dimensional evaluations (micro-CT imaging) as well as functional assessments (biomechanical testing and functional simulations) were done at days 10, 14, and 21 after implant installation. For evaluating the safety profile, the bone defect was filled with 5.5×10^8 pfu/ml Ad-PDGF-B, 5.5×10^9 pfu/ml Ad-PDGF-B, or collagen matrix alone. The hematology, chemical chemistry, and vector dissemination were evaluated over a period of 35 days (n=6/group/time point).

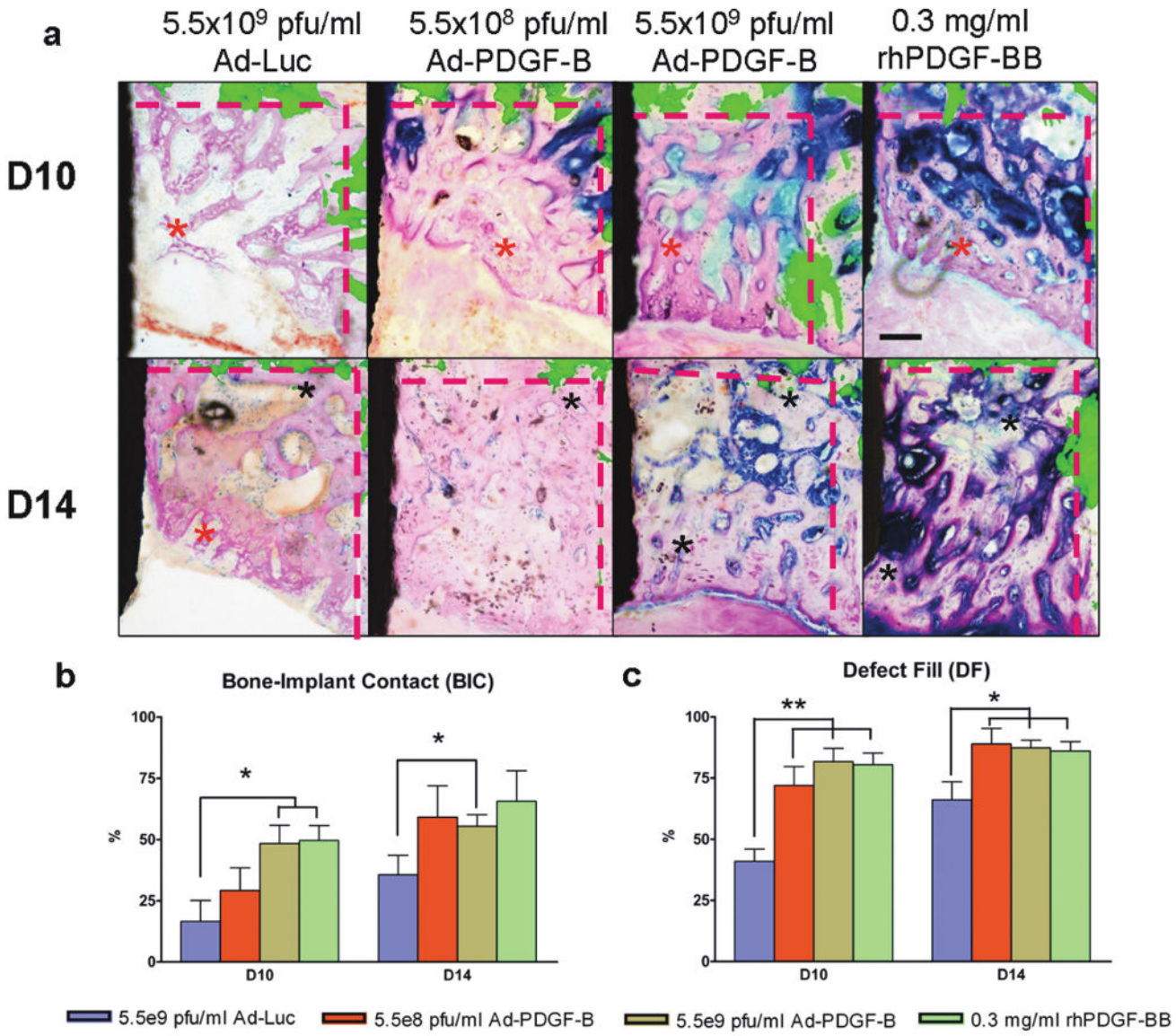

Figure 2. Histologic view of each group for 10 days and 14 days (a) and 2-D evaluations; bone-to-implant contact (BIC) (b), defect fill (c)

(a) Histologic images were overlapped by fluorescent images made by calcein injection 3 days after surgery. The fluorescence indicates the original defect boundaries. The results of Ad-Luc defects shows sparse bone formation at day 10 and a lesser degree of bone maturation at 10 and 14 days. All the PDGF-related specimens showed increased new bone formation at 10 and 14 days compared to Ad-Luc group. Scale bar in top right panel represents 200 μm. (Original magnification: ×40). (**b**) In BIC analysis, 5.5×10^9 pfu/ml Ad-PDGF-B and rhPDGF-BB groups showed significantly higher ratio than the control group at 10 days and 5.5×10^9 pfu/ml Ad-PDGF-B showed significantly higher ratio than control group at 14 days. (**c**) In defect fill analysis, all three PDGF treatment groups showed higher fractions than Ad-Luc treated defects at 10 and 14 days. Black area in left side: dental implant, black asterisks; matured new bone, red asterisks; young new bone, and dashed line;

borders of the osseous defect. Data are presented as mean and bars indicate standard error measurement (n=6-8).* $p<0.05$, ** $p<0.01$, *Abbreviations: BIC: bone to implant contact*.

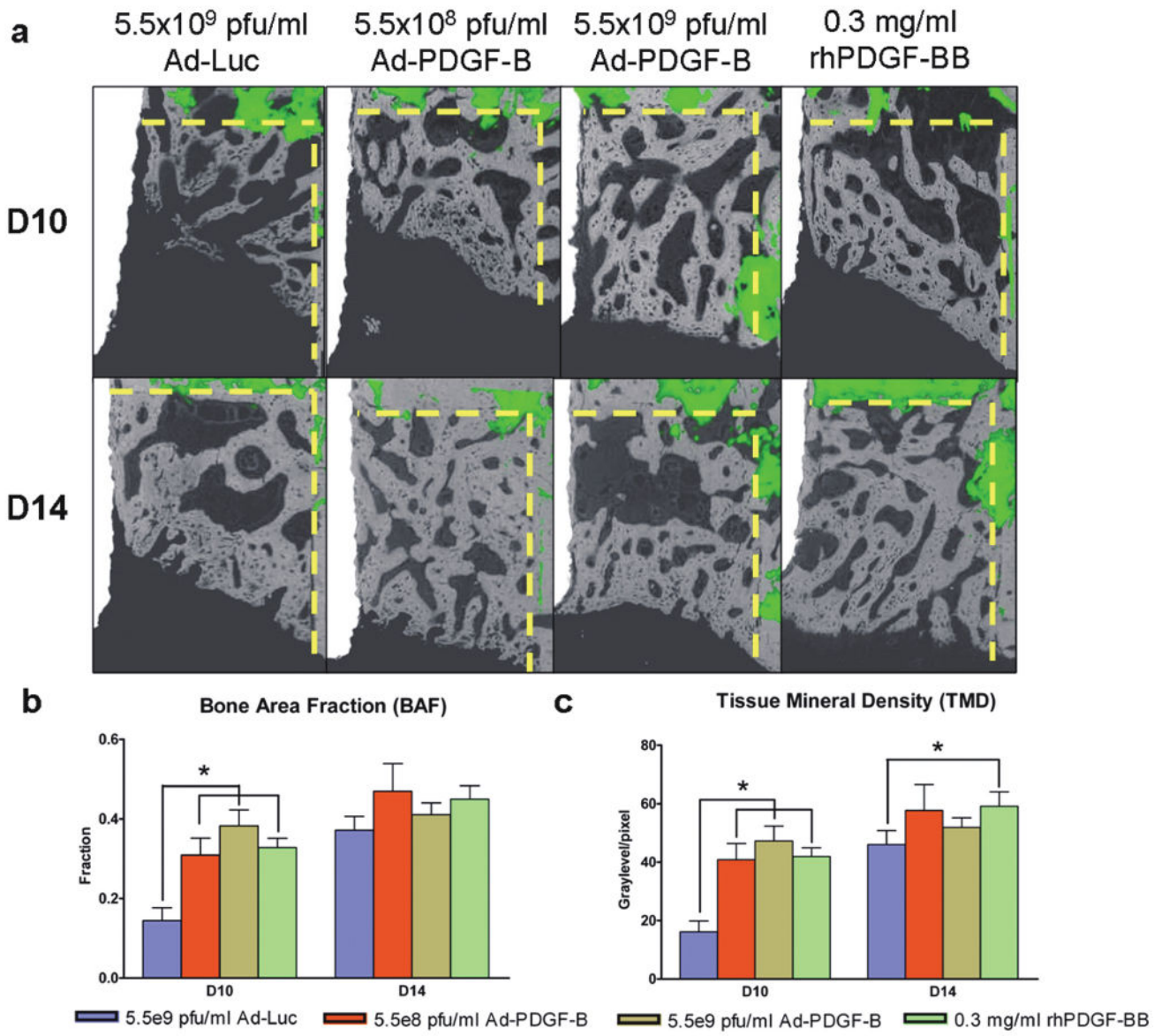

Figure 3. Back scattered SEM (BS-SEM) images (a) and 2-D evaluations; bone area fraction (b), and tissue mineral density (c)

(**a**) BS-SEM images were merged with fluorescent images (dashed line; borders of the osseous defect.). The BS-SEM images show mineralized tissue against the oral implant surface. (Original magnification: ×42) (**b**) The three PDGF treatment groups showed a significant difference in bone area fraction at 10 days compared to the control group. (**c**) The three PDGF groups also showed significant differences in tissue mineral density at 10 days and the rhPDGF-BB group showed significance at 14 days compared to Ad-Luc defects. Data are presented as mean and bars indicate standard error measurement (n=6-8). * $p<0.05$.

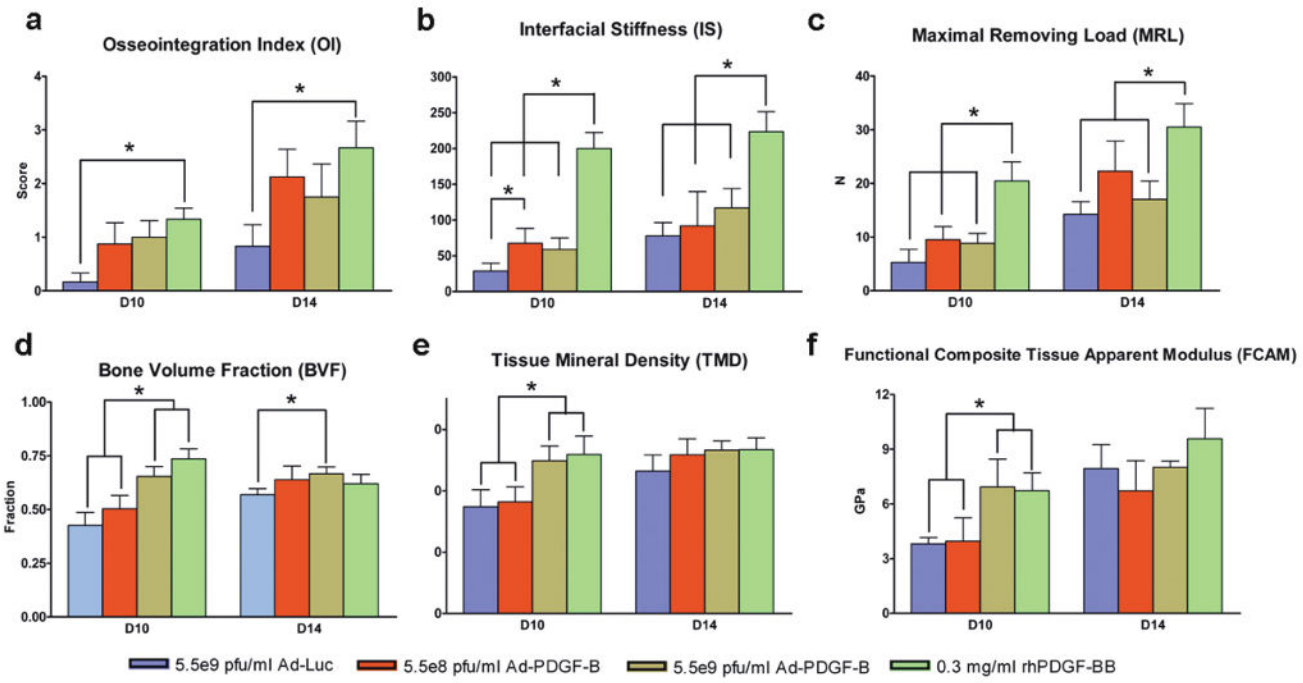

Figure 4. Biomechanical and microCT/functional stimulations demonstrate that Ad-PDGFB and PDGF-BB improve osseointegration *in vivo*

Osseointegration index (**a**), Interfacial stiffness (**b**), maximum removing load (**c**), showed significant differences between rhPDGF-BB treatment and the other three groups. Bone volume fractions (**d**), tissue mineral density (**e**), and functional tissue modulus (**f**) demonstrate that 5.5×10^9 pfu/ml Ad-PDGF-B and rhPDGF-BB displayed significant differences compared to 5.5×10^8 pfu/ml AD-PDGF-B and Ad-Luc groups. There were no significant differences in tissue mineral density and functional composite tissue apparent modulus at day 14. Data are presented as mean and bars indicate standard error measurement (n=6-8). * $p<0.05$, *Abbreviations: FCAM: functional composite tissue apparent modulus*.

Table 1

Hematological analyses for Ad-PDGF-B delivery *

Hematological Parameters	Prior to surgery			Day3			Day 7			Day 14		
	Col	L-Ad	H-Ad	Col	L-Ad	H-Ad	Col	L-Ad	H-Ad	Col	L-Ad	H-Ad
WBC (K/μl)	11.87 (2.99)	10.55 (1.58)	12.15 (2.69)	9.67 (2.82)	11.04 (1.49)	11.81 (1.67)	14.70 (5.22)	11.97 (4.44)	12.15 (2.78)	10.90 (3.98)	11.36 (3.02)	12.23 (3.25)
Neutrophil (K/μl)	2.988 (0.909)	2.462 (0.914)	3.512 (0.995)	2.807 (1.161)	4.542 (1.397)	3.323 (0.778)	4.438 (1.994)	4.340 (2.913)	3.887 (0.878)	3.343 (1.600)	4.547 (2.489)	3.527 (1.272)
Lymphocyte (K/μl)	8.160 (1.355)	7.487 (0.699)	7.840 (1.511)	6.452 (2.962)	5.943 (0.918)	7.768 (1.391)	9.400 (3.051)	6.905 (1.234)	7.658 (2.086)	6.933 (2.103)	6.162 (0.785)	7.988 (1.845)
Monocyte (K/μl)	0.635 (0.311)	0.560 (0.139)	0.550 (0.179)	0.305 (0.091)	0.488 (0.128)	0.648 (0.147)	0.643 (0.299)	0.707 (0.128)	0.493 (0.307)	0.537 (0.307)	0.593 (0.227)	0.540 (0.147)
Eosinophil (K/μl)	0.073 (0.039)	0.048 (0.019)	0.190 (0.158)	0.100 (0.082)	0.058 (0.034)	0.057 (0.028)	0.165 (0.128)	0.157 (0.224)	0.102 (0.122)	0.085 (0.060)	0.048 (0.018)	0.160 (0.118)
Basophil (K/μl)	0.007 (0.012)	0.003 (0.005)	0.052 (0.064)	0.015 (0.023)	0.015 (0.023)	0.007 (0.010)	0.055 (0.053)	0.035 (0.067)	0.002 (0.004)	0 (0)	0.007 (0.010)	0.013 (0.014)
RBC (M/μl)	8.713 (0.305)	8.315 (0.405)	7.388 (0.783)	8.033 (0.585)	8.300 (0.893)	8.082 (0.449)	7.558 (0.493)	7.502 (0.329)	7.925 (0.344)	7.277 (1.257)	7.933 (0.701)	7.963 (0.492)
Hb (g/dl)	16.03 (0.56)	15.53 (0.40)	15.20 (0.64)	15.05 (0.62)	15.13 (1.72)	14.63 (0.78)	13.85 (1.07)	13.65 (0.46)	14.38 (0.58)	14.37 (1.86)	15.68 (1.42)	14.67 (0.23)
Hct (%)	51.68 (2.22)	48.27 (2.76)	42.97 (4.51)	47.50 (3.68)	48.033 (4.88)	47.88 (2.31)	45.02 (3.14)	43.60 (1.71)	47.32 (1.88)	43.95 (8.27)	46.77 (4.35)	48.23 (2.15)
MCV (fl)	59.33 (2.25)	58.07 (1.47)	58.18 (1.64)	59.13 (2.29)	57.90 (1.56)	59.30 (1.43)	59.58 (2.23)	58.20 (0.85)	59.72 (1.59)	60.25 (2.48)	58.97 (2.05)	60.65 (1.72)
MCH (pg)	18.42 (0.74)	18.70 (0.87)	20.77 (2.30)	18.78 (0.89)	18.27 (1.15)	18.13 (0.64)	18.33 (1.14)	18.23 (0.74)	18.13 (0.55)	19.92 (1.40)	19.77 (0.38)	18.47 (1.18)
MCHC (g/dl)	31.05 (0.94)	32.25 (1.59)	35.68 (3.79)	31.75 (1.47)	31.52 (1.64)	30.53 (0.55)	30.77 (1.07)	31.30 (1.07)	30.40 (0.26)	33.12 (2.95)	33.55 (0.81)	30.47 (1.49)
RDW (%)	14.05 (0.42)	13.97 (0.53)	14.10 (0.57)	14.23 (0.49)	14.25 (0.72)	14.10 (0.64)	15.27 (0.72)	15.05 (0.88)	14.50 (0.59)	15.90 (0.43)	15.77 (0.55)	15.55 (0.38)

* All comparisons to collagen group.

n=6/group. The number in this table demonstrates the average value of parameters from the each group and the number in the parentheses refers to the standard deviations. Neither significant differences nor value out of normal range were noted among the Ad-PDGF-B and collagen matrix groups during early time points, as well as beyond 14 days (data not shown). *Abbreviations used: Col:collagen matrix only group, L-Ad: 5.5×10^8 PFU/ml Ad-PDGF-B treated group, H-Ad: 5.5×10^9 PFU/ml Ad-PDGF-B treated group; WBC: white blood cells; RBC: red blood cells; Hb: hemoglobin; Hct: hematocrit; MCV: mean corpuscular volume; MCH: mean corpuscular hemoglobin; MCHC: mean corpuscular hemoglobin concentration; RDW: red blood cell distribution width*

Table 2

Clinical chemical analyses for Ad-PDGF-B delivery *

Clinical Chemical Parameters	Prior to surgery			Day3			Day 7			Day 14		
	Col	L-Ad	H-Ad	Col	L-Ad	H-Ad	Col	L-Ad	H-Ad	Col	L-Ad	H-Ad
Albumin (g/dl)	2.900 (0.200)	3.100 (0.210)	2.750 (0.055)	2.733 (0.216)	2.783 (0.223)	2.917 (0.223)	2.667 (0.216)	2.600 (0.126)	2.917 (0.117)	2.750 (0.243)	2.700 (0.420)	2.783 (0.194)
ALP (U/l)	200.67 (29.49)	253.50 (28.81)	207.50 (36.30)	183.67 (45.70)	195.50 (45.05)	141.17 (30.64)	177.83 (41.80)	163.50 (28.39)	192.17 (40.63)	204.00 (46.43)	227.83 (51.34)	200.00 (36.78)
ALT (U/l)	89.67 (7.74)	88.17 (6.68)	90.33 (8.55)	75.00 (8.60)	76.67 (13.31)	69.50 (3.78)	87.50 (22.82)	85.50 (7.23)	89.83 (15.96)	85.83 (10.46)	78.83 (8.11)	89.67 (11.27)
Amylase (U/l)	2182.17 (119.59)	2054.5 (333.84)	2019.67 (209.93)	1706.67 (256.08)	1335.00 (246.33)	1487.50 (155.96)	1779.00 (189.74)	1589.50 (232.52)	1764.17 (188.13)	1893.17 (226.83)	1742.00 (504.32)	1945.67 (219.46)
AST (U/l)	81.33 (16.67)	78.33 (9.42)	80.83 (12.95)	91.50 (12.42)	115.00 (42.68)	88.33 (17.10)	97.83 (23.70)	71.50 (10.88)	98.00 (11.51)	73.00 (9.38)	85.50 (10.58)	83.50 (14.15)
Bilirubin (mg/dl)	19.67 (1.37)	21.83 (1.47)	23.33 (1.86)	23.33 (2.25)	24.00 (1.67)	20.67 (1.03)	21.67 (1.63)	19.33 (1.03)	22.83 (1.47)	21.67 (1.86)	29.67 (14.60)	22.33 (2.07)
Calcium (mg/dl)	11.18 (0.70)	10.78 (0.23)	10.63 (0.15)	10.28 (0.16)	10.32 (0.23)	10.60 (0.23)	10.47 (0.22)	10.57 (0.29)	10.35 (0.25)	10.52 (0.22)	10.58 (0.26)	10.80 (0.27)
Cholesterol (mg/dl)	87.17 (17.97)	87.50 (13.07)	81.00 (7.69)	99.33 (14.31)	106.83 (13.12)	95.33 (7.31)	83.00 (20.95)	83.83 (9.81)	82.33 (7.45)	90.50 (17.07)	93.17 (16.10)	84.33 (15.34)
Creatine Kinase (U/l)	105.83 (11.86)	94.67 (12.04)	104.50 (36.54)	426.5 (72.45)	403.50 (146.06)	153.00 (119.30)	302.50 (132.63)	115.67 (55.85)	346.33 (117.08)	83.50 (35.80)	244.83 (110.49)	94.83 (22.48)
Creatinine (mg/dl)	0.283 (0.041)	0.383 (0.041)	0.383 (0.041)	0.383 (0.041)	0.400 (0.063)	0.333 (0.082)	0.433 (0.234)	0.367 (0.052)	0.400 (0)	0.350 (0.055)	1.700 (3.184)	0.400 (0)
Glucose (mg/dl)	181.00 (18.98)	187.33 (3.44)	283.33 (52.30)	225.17 (48.06)	251.00 (77.69)	226.33 (39.62)	243.17 (127.82)	275.83 (33.58)	209.83 (23.20)	255.83 (58.81)	223.83 (62.07)	295.83 (40.92)
Phosphorus (mg/dl)	5.983 (0.313)	5.767 (0.497)	5.300 (0.498)	5.567 (0.383)	5.533 (0.524)	5.700 (0.704)	5.733 (0.625)	5.250 (0.367)	5.983 (0.417)	5.700 (0.228)	6.500 (1.942)	5.467 (0.372)
T. Bilirubin (mg/dl)	0.167 (0.052)	0.117 (0.041)	0.167 (0.082)	0.117 (0.041)	0.217 (0.240)	0.400 (0.642)	0.250 (0.207)	0.167 (0.103)	0.183 (0.075)	0.200 (0.155)	0.150 (0.122)	0.217 (0.117)
Total Protein (g/dl)	6.517 (0.256)	6.550 (0.217)	6.017 (0.117)	6.217 (0.343)	6.267 (0.344)	6.467 (0.484)	6.233 (0.207)	5.850 (0.207)	6.300 (0.141)	6.183 (0.204)	6.150 (0.689)	6.067 (0.314)
Globulin (g/dl)	3.617 (0.407)	3.483 (0.041)	3.283 (0.147)	3.467 (0.186)	3.483 (0.133)	3.567 (0.273)	3.533 (0.695)	3.250 (0.152)	3.400 (0.632)	3.383 (0.117)	3.560 (0.114)	3.300 (0.141)

*All comparisons to collagen group.

n=6/group. The number in this table demonstrates the average value of parameters from the each group and the number in the parentheses refers to the standard deviations. Neither significant differences nor value out of normal range were noted among the Ad-PDGF-B and collagen matrix groups during early time points, as well as beyond 14 days (data not shown). *Abbreviations used: Col:collagen matrix only group, L-Ad: 5.5×10^{8} PFU/ml Ad-PDGF-B treated group, H-Ad: 5.5×10^{9} PFU/ml Ad-PDGF-B treated group; ALP: alkaline phosphatase; ALT: alanine transaminase; AST: aspartate transaminase; T. Bilirubin: total bilirubin*